Osteolineage niche cells initiate hematopoietic stem cell mobilization

Shane R. Mayack[1] and Amy J. Wagers[1]

[1]Section on Developmental and Stem Cell Biology, Joslin Diabetes Center, Department of Stem Cell and Regenerative Biology, Harvard University, and Harvard Stem Cell Institute, Boston, MA

Recent studies have implicated bone-lining osteoblasts as important regulators of hematopoietic stem cell (HSC) self-renewal and differentiation; however, because much of the evidence supporting this notion derives from indirect in vivo experiments, which are unavoidably complicated by the presence of other cell types within the complex bone marrow milieu, the sufficiency of osteoblasts in modulating HSC activity has remained controversial. To address this, we prospectively isolated mouse osteoblasts, using a novel flow cytometry–based approach, and directly tested their activity as HSC niche cells and their role in cyclophosphamide/granulocyte colony-stimulating factor (G-CSF)–induced HSC proliferation and mobilization. We found that osteoblasts expand rapidly after cyclophosphamide/G-CSF treatment and exhibit phenotypic and functional changes that directly influence HSC proliferation and maintenance of reconstituting potential. Effects of mobilization on osteoblast number and function depend on the func-tion of ataxia telangiectasia mutated (ATM), the product of the *Atm* gene, demonstrating a new role for ATM in stem cell niche activity. These studies demonstrate that signals from osteoblasts can directly initiate and modulate HSC proliferation in the context of mobilization. This work also establishes that direct interaction with osteolineage niche cells, in the absence of additional environmental inputs, is sufficient to modulate stem cell activity. (Blood. 2008;112:519-531)

Introduction

Mature blood cells have a finite lifespan that necessitates their constant replenishment from self-renewing, multipotent hematopoietic stem cells (HSCs).[1] HSC maintenance and expansion are thought to be regulated by interactions with bone marrow (BM) stromal elements, including osteoblasts[2-4] and vascular endothelial cells,[5] both of which have been proposed to form a supportive HSC "niche."[2,6-8] Osteoblasts, in particular, have been implicated in controlling HSC numbers, and studies in gene-targeted[2] and hormone-treated[6,9] mice show a strong correlation between experimentally induced expansion of osteoblasts and increased HSC frequency. Significantly, most studies of osteoblast function as it relates to HSC have relied on complex in vivo models[10-13] or on in vitro systems in which osteoblasts are derived ex vivo by extended culture of calvarial precursor cells.[10] Although clearly suggestive, these in vivo analyses are complicated by the unavoidable presence of other, nonosteoblastic cell types, whereas in vitro studies of culture-derived osteoblasts are challenged by the possibility that extended culture may induce changes in osteoblast behavior and/or may fail to properly recapitulate the in vivo conditions under which osteoblasts normally would be formed or regulated. For these reasons, it has been difficult to establish the particular aspects of HSC function that depend on the osteoblastic niche, and this has generated significant controversy regarding the specific role of osteoblasts in HSC regulation.[5,14,15]

To overcome these earlier complications, in this study, we develop and use a novel strategy to prospectively isolate mouse osteoblasts and test the function of these cells as regulatory niche cells for HSCs. Through a battery of phenotypic and functional assays, we demonstrate that osteoblasts can be prospectively identified and purified by fluorescence-activated cell sorting (FACS) from marrow-depleted, enzymatically treated mouse bones. Using this direct approach, we further demonstrate that, in response to pharmacologic mobilization, increases in the in vivo frequency and numbers of prospectively identified osteoblasts immediately precede parallel increases in the frequency and number of HSC, suggesting that increased niche availability may enable stem cell expansion in response to mobilization. Finally, we show that freshly isolated osteoblasts from either untreated or mobilized mice can communicate directly with HSCs and are themselves sufficient to induce physiologically relevant changes in HSC function, and that this function depends, at least in part, on the protein kinase ataxia telangiectasia mutated (ATM). In particular, short-term in vitro exposure assays indicate that normal osteoblasts maintain HSC function in part by holding them in a quiescent state through direct cell-cell contact, whereas mobilizing agents induce changes in osteoblastic niche cells that cause them to elaborate soluble factors that instead promote HSC proliferation while maintaining their functional reconstituting potential. Interestingly, these mobilization-induced changes in both osteoblast number and support of HSC function are diminished in the absence of ATM, a kinase previously implicated in regulating oxidative stress,[16-18] inflammation,[19,20] bone remodeling,[21] and stem cell self-renewal.[22-24]

Together, these data underscore the importance of the HSC microenvironment in determining HSC activity and highlight the dynamic nature of the HSC niche. Moreover, by using purified cell populations, this study provides the first clear evidence that direct interactions between hematopoietic precursors and osteolineage niche cells, without any other environmental inputs, are sufficient

---

to specifically modulate HSC number and function. The capacity of purified osteoblasts to act as autonomous regulators of HSC activity in vitro further establishes a new and powerful system that for the first time permits direct interrogation of the interactions of stem cells with their niche and reveals novel and fundamental aspects of stem cell regulation that will improve our understanding of the environmental influences controlling stem cell activity in both normal and pathologic settings. These environmental inputs might be directly exploited for future therapeutic application to a number of hematologic diseases.

Methods

Mice

Wild-type C57Bl/Ka and C57Bl/6 transgenic mice constitutively expressing cyan fluorescent protein (CFP) driven by the ubiquitous β-actin promoter[25,26] and ATM-deficient mice (kindly provided by Fred Alt, Harvard Medical School) were bred and maintained at the Joslin Diabetes Center (C57Bl/Ka, C57Bl/6, and CFP) or Harvard School of Public Health (ATM). Animals used in transplantation studies were bred and maintained at the Harvard School of Public Health. Mice were housed under specific pathogen-free conditions and were generally killed at 8 to 10 weeks of age. All procedures were approved by the Institutional Animal Care and Use Committee.

Antibodies and flow cytometry

The antibodies used in these studies included 19XE5 (α-Thy1.1 phycoerythrin [PE] conjugate), 2B8 (α-c-kit Pacific Blue conjugate), E13-161.7 (α-Sca-1, Ly6A/E, allophycocyanin [APC] conjugate), ZH2 (rat α-osteopontin, unconjugated, Chemicon International, Temecula, CA), rat α-IgG (fluorescein isothiocyanate [FITC] conjugate), Ter119 (α-erythrocyte-specific antigen, Ly-76, APC-Cy7 conjugate), 30-F11 (α-CD45, APC-Cy7 conjugate). Lineage marker antibodies included the following biotinylated antibodies: KT31.1 (α-CD3), GK1.5 (α-CD4), 53-7.3 (α-CD5), Ter119 (α-erythrocyte-specific antigen, Ly-76), 6B2 (α-B220), 8C5 (α-Gr-1), and M1/70 (α-Mac-1) and streptavidin APC-Cy7 was used as the secondary antibody. Annexin V (APC conjugate) was used in apoptosis assays on cultured hematopoietic progenitors cells and ATM-deficient osteoblasts. Antibodies were from eBioscience (San Diego, CA) unless otherwise noted. Cells (2×10^{-6}/100 μL) were stained with corresponding antibodies for 10 minutes in Hank buffered saline solution (HBSS) supplemented with 2% donor bovine serum. For annexin V staining, cells were washed in annexin V staining buffer (0.01 M HEPES [N-2-hydroxyethylpiperazine-N′-2-ethanesulfonic acid], pH 7.4, 0.14 M NaCl, 2.5 mM CaCl) after first staining for cell surface markers, and then incubated with annexin V–specific antibody (5 μL/100 μL) for 15 minutes. Propidium iodide (PI) was used as a marker for cell viability and added to samples just before sample acquisition. Flow cytometric experiments were performed using an LSRII, FACS-Aria (BD Biosciences, San Jose, CA) or Moflo (Dako North America, Carpinteria, CA). Data were analyzed with FlowJo software (TreeStar, Ashland, OR) and represented as histograms, contour, or dot plots of fluorescence intensity.

BM cell and osteoblast isolation

Total BM cells were isolated from mouse femurs and tibias by flushing with HBSS plus 2% fetal bovine serum (FBS). Red blood cells and debris were removed by ACK lysis (Ammonium chloride lysis: 0.15 M NH4Cl, 1.0 mM KHCO3, 0.1 mM EDTA, pH 7.4) and filtering through nylon mesh. Osteoblasts were isolated from marrow-depleted bones by mechanical disruption (crushing with mortar and pestle) and enzymatic digestion in 0.1% collagenase plus 0.05% dispase for 1 hour. Bone-associated cells liberated by enzymatic treatment were collected by centrifugation (5 minutes, 400g).

Quantitative RT-PCR

Equivalent numbers of OPN+CD45−Ter119−, OPN−, or total BM cells were isolated as described in "BM cell and osteoblast isolation," and total RNA was prepared by sorting cells directly into TRIZOL reagent (Invitrogen, Carlsbad, CA) and following the manufacturer's specifications. Total RNA was treated with DNAse I to remove contaminants and used for RT according to the manufacturer's instructions (Superscript II kit, Invitrogen). Polymerase chain reaction (PCR) reactions were performed in an ABI-7000 detection system using SYBR green PCR Core Reagents (Applied Biosystems, Foster City, CA). PCR amplification was performed in a 10-μL final volume containing 1 X SYBR Green PCR buffer, 2 mM of MgCl2, 0.5 mM of dNTPs, 10 ng of each primer, 0.25 U of AmpliTaq Gold and 1 μL of cDNA templates. β-Actin gene expression was used to normalize the amount of each investigated transcript. For primer sequences and PCR cycling conditions, see Figure S6 (available on the Blood website; see the Supplemental Materials link at the top of the online article). For single-cell RT-PCR, single OPN+CD45−TER119− cells were twice-sorted by FACS and deposited directly into 96-well PCR plates containing 19 μL of RT lysis buffer (50 mM Tris-HCl, pH 8.0, 100 mM NaCl, 5 mM MgCl2, 0.5% Triton X-100, 1 mM dithiothreitol, and 100 units RNasin Ribonuclease inhibitor/mL buffer). This was followed immediately by centrifugation, and reverse-transcription (RT)-PCR analysis was performed according to standard protocols as described. The contents of each well were reverse transcribed in the presence of oligo-dT and random hexamer and the final cDNA product of each well was divided equally for amplification with gene specific primers.

ELF-97 alkaline phosphatase assays

Alkaline phosphatase (ALP) activity was measured using the ELF-97 Endogenous Phosphatase Detection Kit (Invitrogen) per the manufacturer's instructions with a modification for flow cytometric analysis as described previously.[27] Isolated osteoblasts were washed twice in 0.15 M normal saline solution without phosphate buffers. The ELF-97 phosphate substrate was added to cells preincubated in ELF-97 developing buffer (15 minutes) in a final volume of 100 μL (1:20 in provided buffer). Cells were incubated in the dark at room temperature for 1 to 30 minutes, followed by the addition of the phosphatase inhibitor levamisole (10 mM) to all tubes to stop the reaction. The cells were then analyzed by flow cytometry (Moflo, Dako North America) within 1 hour.

Bone nodule assays

OPN+ cells were plated at a density of 10 cells per well in a 96-well plate containing α-MEM supplemented with 15% FBS, 100 U/mL penicillin, and 1 mg/mL streptomycin. On day 15 of culture, ascorbic acid (20 mg/mL) and β-glyceraldehyde (50 μM) were added to each well. Seven days (d22 after culture start) and 15 days (d30 after culture start) after addition of ascorbic acid and β-glyceraldehyde, cultures were screened for bone nodule formation as well as ALP gene expression and activity. To detect mineralization of bone nodules, cell cultures were stained with 1% silver nitrate (von Kossa method). Briefly, the cell cultures were washed twice with phosphate-buffered saline (PBS), fixed in phosphate-buffered formalin for 10 minutes, washed once with water, and serially dehydrated in 70%, 95%, and 100% EtOH 2 times each and air dried. The plates were then rehydrated from 100% to 95% to 80% EtOH to H2O. The water was removed, a 1% silver nitrate solution was added, and the plate was exposed to light for 20 minutes after which the plate was rinsed with water. Sodium thiosulfate (5%) was added for 3 minutes and rinsed with water; mineral was stained dark red to black. Plates were viewed with an Olympus IX 51 inverted research microscope (Olympus America, Melville, NY) using either a UPLan FL N lens at 4×/0.13 or a UPLanF1 lens at 10×/0.30 Ph1 (Olympus America, Melville, NY). All images were acquired using a Microfire Digital CCD camera model no. 599809 (Optronics, Goleta, CA) and were processed with Picture Frame Imaging software version 2.3 (Optronics, Goleta, CA) and Adobe Photoshop version 7.0 software (Adobe Systems, San Jose, CA).

Cy/G treatment, in vivo BrdU administration, and BrdU staining

Mobilization of HSCs by combined administration of cyclophosphamide (Cy) and granulocyte-colony stimulating factor (G-CSF) was performed as described previously.[28] For in vivo bromodeoxyuridine (BrdU) cell labeling, BrdU was administered by intraperitoneal injection (1 mg/mL) as a repeated dose every 12 hours, for all experimental groups (untreated, D0, D2, D4), beginning 12 hours after experimental group D4 received Cy. To measure BrdU incorporation, osteoblasts were first stained with antibodies to cell surface epitopes (CD45, Ter119, and OPN). After initial staining, cells were fixed in 70% ethanol overnight at 4°C, denatured in 2N HCL/0.5% Triton X-100 for 30 minutes at room temperature, neutralized with 0.1 M sodium borate (pH 8.5) for 5 minutes, and stained with anti-BrdU FITC-conjugated antibody (BD Biosciences) for 30 minutes at room temperature in PBS/0.5% bovine serum albumin/0.5% Tween 20. Cells were resuspended in 300 μL PBS and analyzed on a FACS LSRII or FACSAria.

Cell culture and proliferation assays

Hematopoietic progenitor cells (HPC, 10^5) and osteoblasts (2×10^3) were isolated as described and cocultured in RPMI supplemented with 10% FBS plus 100 U/mL penicillin and 1 mg/mL streptomycin for 12 or 36 hours as indicated for each experiment. For proliferation assays based on the loss of carboxyfluorescein succinimidyl ester (CFSE), cells were harvested as described and total BM cells were first stained with antibodies for lineage depletion and then incubated with CFSE (5 μM) at a cell density of less than or equal to 10^6/mL for 20 to 30 minutes at 37°C. After staining, cells were washed in HBBS containing 2% FBS, and Lineage⁻ CFSE⁺ HPCs were sorted and cocultured with or without the indicated osteoblast populations. After 12 or 36 hours, cells were harvested and the loss of CFSE within the KTLS (c-Kit⁺Thy1.1ˡᵒLin⁻Sca-1⁺) population was determined by flow cytometric analysis and compared with control populations of HPCs that were left unlabeled (negative control), freshly labeled with CFSE, or CFSE labeled and stored at 4°C for the duration of the experiment (positive control for undivided fraction). For transwell assays, experiments were performed as described except that osteoblasts were cultured in the top well of a transwell chamber and physically separated by a 0.4-μm pore from HPCs present in the bottom well.

Hematopoietic progenitor cell isolation and bone marrow transplantation

HPCs for coculture experiments were isolated from WT (for CFSE studies), CFP⁺ (for mobilized osteoblast transplant studies), or GFP⁺ (for ATM-deficient osteoblast transplant studies) mice by lineage depletion of BM using a cocktail of biotinylated primary antibodies (CD3, CD4, CD5, B220, Ter119, Gr-1, and Mac-1). Cells negative for all the mature hematopoietic markers were considered lineage negative (Lin⁻) BM-derived HPCs and were sorted by FACS. For transplantation, approximately 5000 HPCs were given intravenously by retro-orbital injection to lethally irradiated mice (950 cGy, immediately before transplantation) along with 3×10^5 unfractionated whole BM cells as helper cells. Multilineage engraftment (percentage of donor-derived mature hematopoietic cells) was monitored by FACS analysis of peripheral blood collected via tail vein 4, 6, 8, 10, and 16 weeks after transplantation. Blood leukocytes were stained with antibodies specific for the myeloid (Mac-1-PE, Gr-1-PE), B-cell (B220-Alexa750-APC) and T-cell (CD3-, CD4-, CD8-PE-Cy7 antibody cocktail) compartments (all antibodies from eBioscience), and the frequency of donor-derived cells within each of these populations was determined after exclusion of all red blood cells (by Ter119-PE-Cy5) and dead cells (by PI⁺). Because CFP⁺ transgenic mice express the transgene in only a subset of peripheral blood leukocytes (80%-90%), donor-derived chimerism (CFP⁺ cells) in transplanted animals was normalized based on the frequency of CFP expression in mature peripheral blood populations isolated from unmanipulated CFP⁺ animals.

Statistical analysis

Results are expressed as means plus or minus SD. Data were analyzed using the unpaired 2-tailed Student t test or a one-way analysis of variance as appropriate for the data set. P less than or equal to .05 was considered significant.

Results

Osteoblasts can be isolated by direct cell sorting

To facilitate direct studies of osteoblast function in the regulation of homeostatic and regenerative HSC function, we established parameters for flow cytometry-based identification and isolation of bone-associated osteoblasts from enzymatically digested bone. Long bones (femurs and tibias) harvested from wild-type C57BL/Ka mice were first depleted of marrow by flushing with a syringe, and then gently crushed with a mortar and pestle to generate approximately 1-mm² "bone chips" (Figure 1A). Adherent bone-associated cells were liberated from the bone chips by digestion with a solution of collagenase/dispase,[29] and single-cell suspensions of bone-associated cells (or BM for comparison) were stained with antibodies against selected cell surface markers and analyzed by flow cytometry. In this search for osteogenic cells, we restricted our analysis to the nonhematopoietic (CD45⁻Ter119⁻) subset of bone-associated cells,[2,6,9,10] and screened this subset for expression of osteoblast-associated cell surface markers (Figure 1B and data not shown). Given that previous studies have demonstrated relatively restricted expression by bone lineage cells of the secreted/cell surface marker osteopontin (OPN),[30-36] and that analyses of OPN⁻/⁻ mice suggest that OPN acts on HSCs to restrict their numbers in vivo,[8,37] we hypothesized that OPN might serve as a useful marker for the identification and isolation of HSC-interacting osteoblastic niche cells. Indeed, flow cytometric analysis revealed the existence of a distinct population of nonhematopoietic (CD45⁻Ter119⁻) cells expressing OPN (OPN⁺), which was present in preparations of enzymatically liberated bone-associated cells but was not detected among BM cells (Figure 1B).

To test whether OPN⁺CD45⁻Ter119⁻ cells were enriched for osteolineage cells, we isolated RNA from FACS-purified OPN⁺CD45⁻Ter119⁻ cells and analyzed the expression of additional osteoblast-specific transcripts, including osteocalcin (OC), bone-specific alkaline phosphatase (ALP), osteoactivin (OA), Runx-2 (RX2), and Osterix (OS) by these cells using real-time PCR.[38,39] Double-sorted populations of bone-associated OPN⁺CD45⁻Ter119⁻ cells showed significantly increased expression (from 1.5- to 8-fold, $P < .05$ for each comparison) of each of these bone-specific markers compared with expression of these genes in total BM cells (which contain primarily hematopoietic lineage cells; Figure 1C top panel) and compared with sorted OPN⁻CD45⁻Ter119⁻ nonosteoblastic BM stromal cells (OPN⁻; Figure 1C top panel). Furthermore, OPN⁺CD45⁻Ter119⁻ cells showed significantly reduced expression of several endothelial markers, compared with both OPN⁻CD45⁻Ter119⁻ nonosteoblastic BM stromal cells and total BM cells. The osteoblast-associated cell surface receptor parathyroid hormone receptor (PTHR1)[40] was also present on the majority of OPN⁺CD45⁻Ter119⁻ cells (Figure 1D, 70% ± 6%), and lacking on most OPN⁻CD45⁻Ter119⁻ cells (Figure S1).

To assess the homogeneity of OPN⁺CD45⁻Ter119⁻ bone-associated cells, we also determined the frequency of expression of osteoblast-specific markers within this population using single-cell quantitative RT-PCR. Individual OPN⁺CD45⁻Ter119⁻ cells
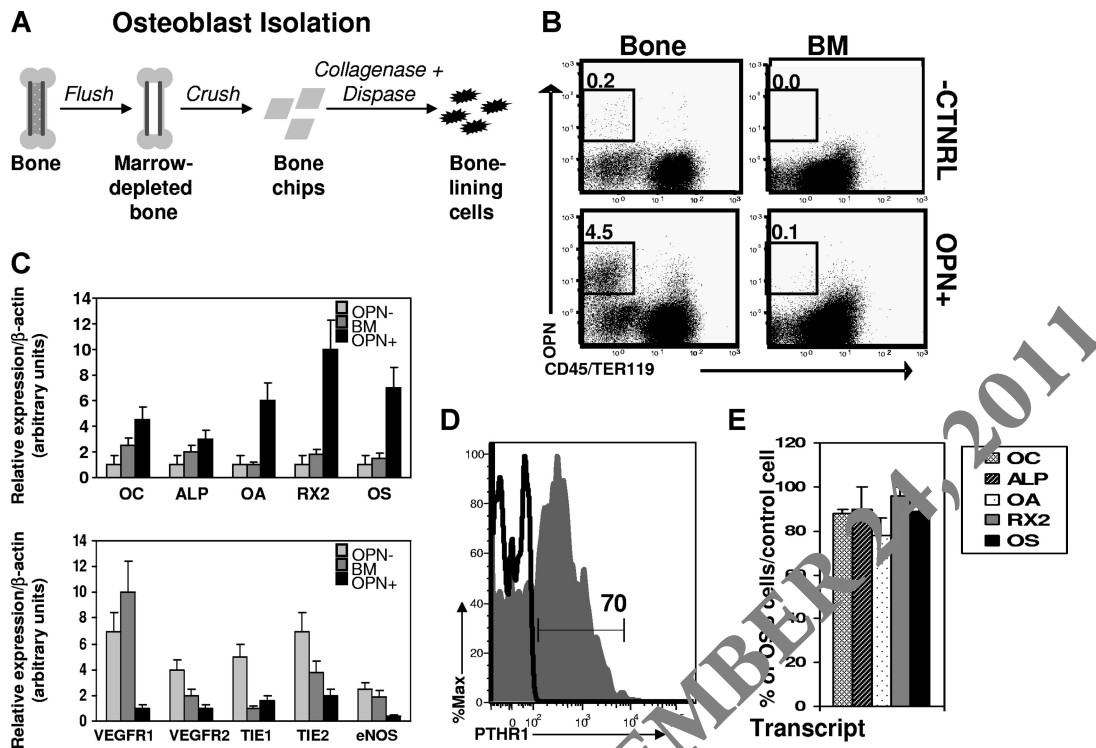
Figure 1. Phenotypic isolation of osteoblasts. (A) Strategy for isolation of bone-associated cells. (B) Flow cytometric analysis of single-cell suspensions from collagenase-treated bone (Bone) or BM aspirates (BM). Data are presented as dot plots showing staining for hematopoietic markers (CD45/Ter119) and Opn. The frequency of Opn$^+$CD45$^-$Ter119$^-$ cells is shown in the upper left. "-CNTRL" indicates representative background fluorescence seen in the absence of Opn secondary antibody (rat-αFITC) or when an isotype control (rat-αIgG) only is used. This is representative of 10 to 15 independent experiments. (C) QRT-PCR analysis of mRNA isolated from double-sorted Opn$^+$ cells (OPN$^+$) compared with irrelevant bone marrow cells (BM) or Opn$^-$ (OPN$^-$) cells. Relative expression (mean ± SD) over a β-actin normalization control is shown for osteocalcin (OC), alkaline phosphatase (ALP), osteoactivin (OA), Runx2 (RX2), and osterix (OS), vascular endothelial growth factor receptor 1 and 2 (VEGFR1, VEGFR2), tyrosine kinase with Ig and EGF homology domains 1 and 2 (TIE1, TIE2), endothelial nitric oxide synthase (eNOS); n = 3 independent experiments for osteolineage markers; n = 2 independent experiments for endothelial markers). Each transcript was measured in triplicate. (D) Flow cytometric analysis of parathyroid hormone receptor-1 (PTHR-1) expression by Opn$^+$CD45$^-$Ter119$^-$ cells (gray histogram) or BM cells (line). Both PTHR1^{hi} and PTHR1^{lo} OPN$^-$CD45$^-$Ter119$^-$ cells exhibited equal levels of activity of bone-specific ALP (Figure S2), consistent with an equivalent state of osteolineage differentiation of PTHR1^{hi} and PTHR1^{lo} cells[12,42] and probably reflecting known differences in PTHR1 expression by functionally equivalent osteoblasts present at local areas of bone formation or of bone resorption.[40] (E) QRT-PCR analysis of mRNA isolated from individual double-sorted Opn$^+$CD45$^-$Ter119$^-$ cells. Data are plotted as the percentage of osteoblasts (mean ± SD) with increased expression of OC, ALP, OA, RX2, or OS compared with a control population of single-sorted total BM cells (n = 2 independent experiments).

were isolated from collagenase-treated bone and subjected to direct expression analysis. The majority of individual OPN$^+$CD45$^-$Ter119$^-$ cells showed elevated expression of all 5 osteoblast markers assessed compared with the levels of these genes expressed by BM cells (OC, 88% vs 12%, $P = .03$; ALP, 90% vs 23%, $P = .004$; OA, 78% vs 10%, $P = .05$; RX2, 96% vs 8%, $P = .004$; OST, 88% vs 5%, $P = .01$; Figure 1E). In addition, OPN$^+$CD45$^-$Ter119$^-$ cells exhibited largely homogeneous expression of several additional cell surface markers examined, including RANKL, CD44, CD51, and VCAM-1, and uniformly lacked expression of several other surface proteins, including markers of the mesenchymal and endothelial lineages (eg, CD43, Sca-1, CD31, and c-Kit; Figure S2).

To further test the osteogenic lineage commitment of sorted OPN$^+$CD45$^-$Ter119$^-$ cells, we assessed the functional activity of this population using 2 standard assays of bone-forming cells: ALP activity and bone nodule formation.[12,31,33,41,42] First, to quantify ALP activity in OPN$^+$CD45$^-$Ter119$^-$ cells, we used the novel phosphatase substrate ELF-97 (Invitrogen). Cells harboring functional ALP are fluorescently labeled by ELF-97 on phosphatase-specific enzymatic hydrolysis, which converts the water-soluble, nonfluorescent ELF-97 substrate to a water-insoluble, fluorescent alcohol that accumulates at the site of enzymatic activity. Incubation of OPN$^+$CD45$^-$Ter119$^-$ cells isolated from collagenase-treated bone with ELF-97 resulted in significant accumulation over

time of a fluorescent signal corresponding to ALP activity (Figure 2A). In contrast, ELF-97-associated fluorescence signal did not increase in a control population of hematopoietic-lineage cells (BM, Figure 2A). Thus, consistent with gene expression analyses (Figure 1), OPN$^+$CD45$^-$Ter119$^-$ cells harbor high levels of functionally active ALP, as expected in a population of osteolineage cells. Significantly, ALP activity was equal among OPN$^+$CD45$^-$Ter119$^-$ cells expressing either high or low levels of PTHR1 (Figure S1A), suggesting that both PTHR1^{hi} and PTHR1^{lo} OPN$^+$CD45$^-$Ter119$^-$ cells are committed osteolineage cells. These data are consistent with a previous study indicating that levels of PTHR expression can vary between otherwise equivalent osteoblast cells present at areas of bone formation as opposed to bone resorption.[40]

Second, as an additional measure of osteoblast function, we also assessed the ability of purified OPN$^+$ cells to form bone nodules in cell culture. Cultures initiated with as few as 10 FACS-purified OPN$^+$ cells were expanded for 15 days and then induced to form bone nodules by the addition of the osteo-inducing agents ascorbic acid and β-glyceraldehyde.[12] Under these conditions, the cultured cells began to form discrete clusters within 7 days (day 22 after culture initiation) and generated distinct nodule-like formations within 15 days (day 30 after culture initiation; Figure 2B). Cells harvested from these cultures exhibited increasing levels of ALP
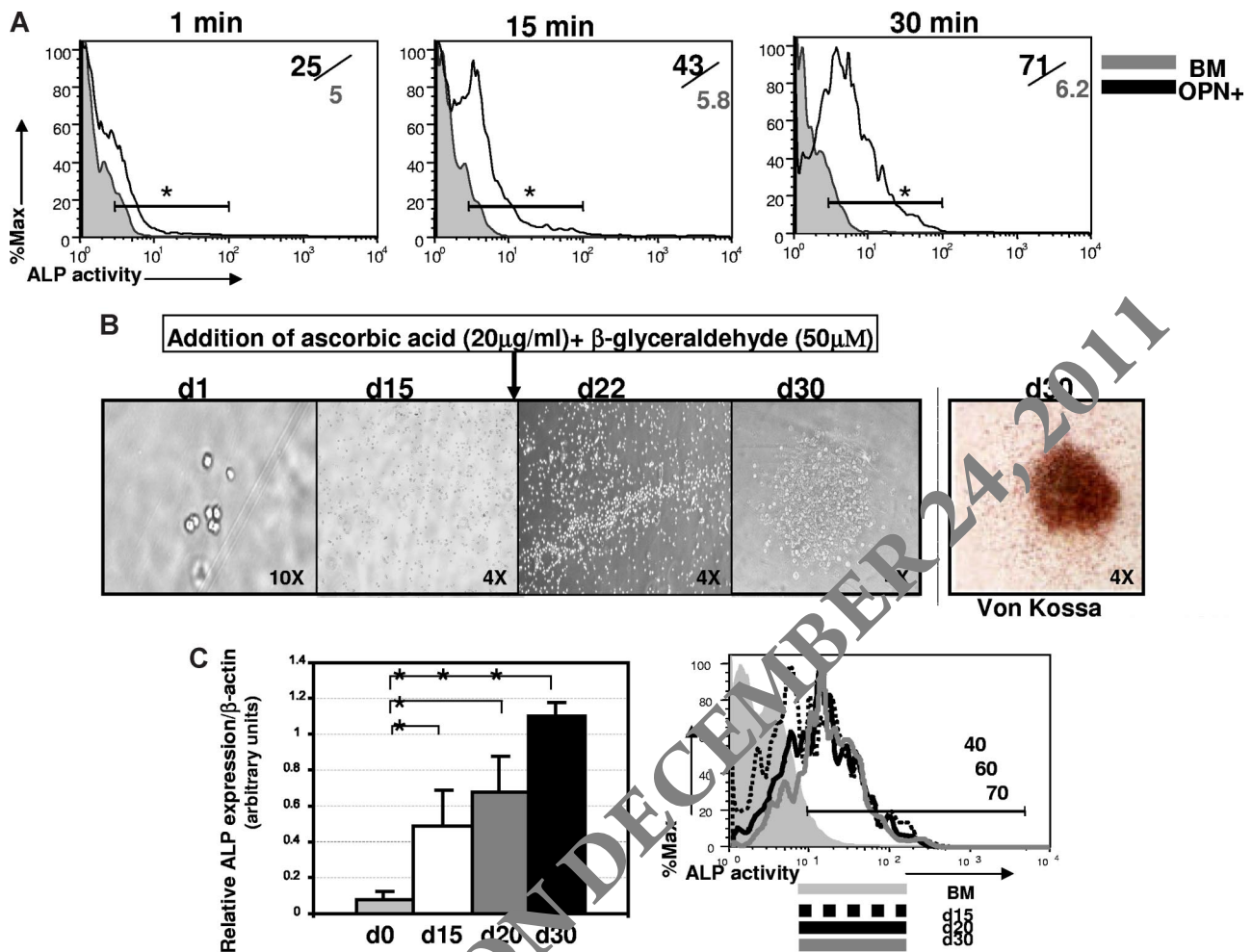
Figure 2. Opn+CD45−Ter119− cells isolated from bone exhibit osteoblast function. (A) Flow cytometric analysis of ALP activity, determined using a modified version of the fluorogenic ELF-97 assay (Invitrogen). Histograms show kinetics (1 minute, 15 minutes, and 30 minutes) of detection of ALP activity in purified Opn+ cells (black line) compared with the ALP activity in a control cell population of total BM cells (gray filled, n = 4). Numbers in the upper right indicate frequency of ALP+ cells among Opn+ cells/frequency of ALP+ among BM control cells. This is representative of 3 independent experiments (*$P <$ .05 at each time point indicated). (B) Sorted osteoblasts form bone nodules in culture. Ten OPN+ cells were cultured in α-MEM/15% serum (d1 of culture, 10 times) and at day 15 (d15, 4 times) osteogenesis was induced by the addition of 20 mg/mL ascorbic acid plus 50 μM β-glyceraldehyde. Cell clusters form after 7 days (d22 of culture, 4 times) and distinct bone nodules are visible by 15 days (d30 of culture, 4 times). Mineralization was confirmed at d30 by the von Kossa method. Micrographs shown are representative of 3 independent experiments (n = 20 wells/experiment). Plates were viewed using a UPLanF1 lens at 10×/0.30 Ph1 (first micrograph) or a UPLan FLN lens at 4×/0.13 (all other micrographs). The efficiency of bone nodule formation was 89% plus or minus 3% of seeded wells over the 3 experiments performed. (C) Differentiating osteoblasts in bone nodule cultures showed increasing expression of ALP mRNA (graph, middle panel, representative of 3 to 5 different wells sampled individually at each time point indicated; *$P <$ .05) and increasing ALP activity (histogram, right panel, representative of 3 individual wells sampled at each time point, day 15, day 20, or day 30, after culture initiation). Data are representative of 3 independent experiments; error bars represent SD

mRNA and increasing ALP activity, consistent with matrix production and progressing osteoblast differentiation (Figure 2C). When stained at 15 days after osteoinduction, nodules derived from sorted OPN+CD45−Ter119− cells exhibited robust mineralization, characteristic of differentiated bone cells, as demonstrated by positive von Kossa staining (Figure 2B last panel).

Taken together, these data demonstrate that sorted OPN+CD45−Ter119− cells exhibit both phenotypic markers and functional properties characteristic of bone lineage cells. FACS thus provides a useful strategy for the direct, prospective isolation of a highly enriched and largely homogeneous population of osteolineage cells. For simplicity, we will hereafter refer to these OPN+CD45−Ter119− cells simply as OPN+ cells. Significantly, this efficient, prospective isolation of osteoblasts by FACS allows a direct assessment of their role as HSC niche cells and their impact on hematopoietic activity in the steady state and after pharmacologic perturbations. We therefore used this novel and powerful approach to directly investigate the

involvement of osteoblasts in HSC proliferation induced by stimulation with stem cell mobilizing agents.

Osteoblasts expand during Cy/G-induced HSC mobilization

HSCs are normally highly quiescent[43,44] and reside primarily in the BM, although they also can be found at low frequency in the circulatory system of normal animals.[45,46] HSC proliferation and migration from the BM to the bloodstream can be dramatically increased by the use of stem cell "mobilizing agents."[28,47] One well-studied regimen for HSC mobilization involves sequential daily treatment with the cytotoxin Cy and the cytokine G-CSF[28,46-48] (Figure 3). After administration of Cy plus 2 daily doses of G-CSF, referred to as day +2 (D2) of the Cy/G regimen (Figure 3A), the BM HSC population exhibits robust proliferation and expansion to numbers 10 to 12 times those seen in untreated mice.[28,44] After D2, HSCs begin to exit the BM and are detected at increased frequency in the blood and peripheral organs by day +3 (D3) and day +4
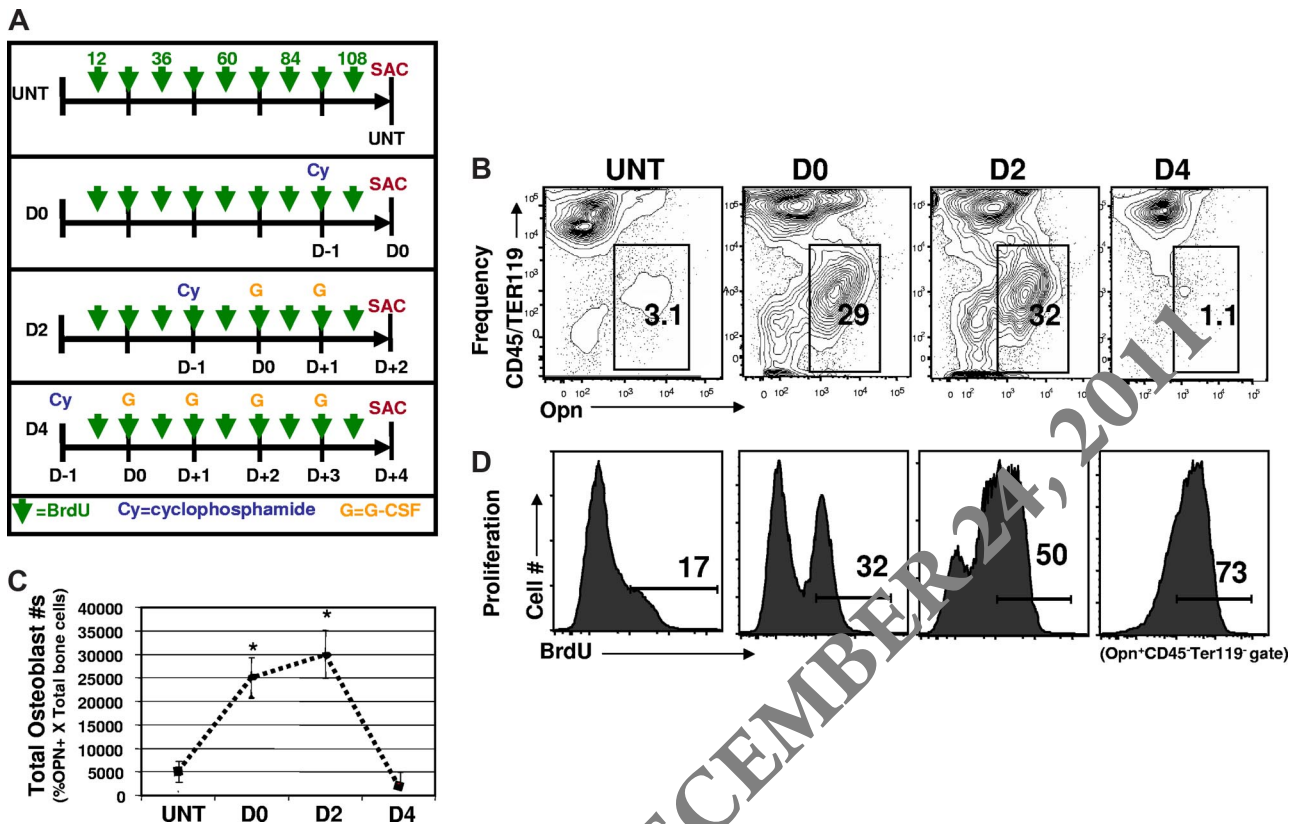
Figure 3. Cy/G-CSF treatment induces changes in the osteoblastic niche. (A) Experimental strategy. For HSC mobilization, mice were injected intraperitoneally with Cy (200 mg/kg) and then on successive days with human G-CSF (250 μg/kg/day) administered as a single daily subcutaneous injection. The day of Cy treatment was considered day −1 and the first day of G-CSF treatment as day 0. The timeline of Cy and G treatments for each experimental group is shown. For in vivo BrdU labeling experiments, mice in every experimental group (untreated, D0, D2, and D4) received 9 successive injections of BrdU (1 mg/mouse in 0.9% saline, intraperitoneally, indicated by green arrows), over a 4.5-day period. All experimental groups began BrdU treatment 12 hours after Cy injection in the first experimental group (D4) and received continued BrdU injections every 12 hours thereafter (indicated by green arrows). Thus, all animals were sacrificed (SAC) after the same time period of BrdU exposure. (B) Osteoblast (Opn$^+$CD45$^-$Ter119$^-$) frequencies are increased in Cy/G-treated mice. Representative FACS plots are shown (n = 10), with the frequency of Opn$^+$CD45$^-$Ter119$^-$ shown in each gate. (C) Total numbers of osteoblasts are increased in response to Cy/G (D2) treatment but return to normal numbers by D4. Data are plotted as means plus or minus SD. Differences were significant for untreated versus D0 (*P < .05) and untreated vs D2 (P < .05). Differences were not significant for untreated versus D4 (*P > .05). (D) Osteoblasts proliferate in response to Cy/G treatment as demonstrated by increased in vivo uptake of BrdU in osteoblasts from mobilized (D0, D2, and D4) as opposed to untreated (untreated, far left) mice. Histograms indicate the percentage BrdU$^+$ cells (determined by control staining of osteoblasts from mice that did not receive BrdU) among Opn$^+$CD45$^-$Ter119$^-$ cells. This is representative of 2 independent experiments.

(D4).[28,47] By D4 of Cy/G treatment, the rate of HSC proliferation in the BM returns approximately to normal, and the population size shrinks to steady-state levels.[28,44]

Given that previous studies in which osteoblast numbers have been experimentally manipulated have suggested that the number and/or availability of these cells may directly regulate the number of HSCs,[2-4,6] we wondered whether the dramatic expansion of HSC that occurs in response to Cy/G treatment might be accompanied by a concomitant expansion of osteoblastic niche cells. To test this possibility, we used flow cytometry to directly enumerate osteoblasts harvested fresh from the long bones of untreated or Cy/G mobilized mice (Figure 3). On Cy/G treatment, both the frequency (Figure 3B) and total number (Figure 3C) of osteoblasts (OPN$^+$CD45$^-$Ter119$^-$ bone-associated cells) isolatable from the long bones increased up to 10-fold, compared with untreated mice. This Cy/G-induced expansion of the osteoblast compartment began at day 0 (D0), in mice receiving Cy only treatment, and continued through D2, in mice receiving Cy + 2 doses of G (Figure 3B); however, osteoblast frequencies and numbers returned to normal (ie, equivalent to the frequency and number of OPN$^+$ cells seen in untreated animals by D4; Figure 3B,C). Precisely how homeostasis is restored to the osteoblast compartment by D4 of Cy/G-treatment remains unclear and is a topic of ongoing investigation.

Interestingly, in contrast to mice treated with Cy/G, in animals receiving G-CSF alone (for 2 days), we observed no detectable increase in the frequency of OPN$^+$ cells (G$_2$, 2% ± 1% OPN$^+$), compared with mice left untreated (untreated, 2.5% ± 2% OPN$^+$; Figure S3). The observation that osteoblasts are not induced by treatment with G-CSF alone is consistent with previous studies[49,50] and correlates with earlier observations that treatment of mice with G-CSF results in only mild expansion of BM HSCs,[47,51] as opposed to the dramatic (10- to 12-fold) expansion of BM HSCs in mice treated with the combination of Cy + G-CSF.[28,46]

To more directly assess changes in the proliferative activity of osteoblasts in Cy/G-treated mice, we also measured incorporation of BrdU by these cells during mobilization treatment. Mice were treated as before with Cy/G and additionally received daily injections of BrdU (1 mg/mL, intraperitoneally) to label dividing cells. BrdU labeling was initiated at the same time for all experimental groups (untreated, D0, D2, D4) and this time point coincided with Cy administration in the first experimental group to begin treatment (12 hours after Cy administration in the D4 experimental group). Labeling was continued for all animals by intraperitoneal injection every 12 hours until the animals were

killed (Figure 3A green arrows). Thus, all animals in this experiment received comparable amounts of BrdU over precisely the same period of time (4.5 days).

As shown in Figure 3D, in untreated mice, few OPN$^+$ cells divided during the 4.5 days of BrdU labeling (17% ± 5% BrdU$^+$). However, Cy/G treatment dramatically increased the rate of osteoblast proliferation over this time period, with 32% plus or minus 4% of isolatable OPN$^+$ cells labeled with BrdU in D0 mice, 50% plus or minus 8% in D2 mice, and 75% plus or minus 6% BrdU$^+$ in D4 mice. These data indicate that Cy/G treatment activates proliferation of osteolineage cells, which leads to substantial increases in osteoblast frequency and absolute numbers. Interestingly, osteoblast expansion appears to precede HSC expansion in the Cy/G model (Figure 3), as HSCs are maximally expanded at D2.[28,47] These data support the notion that the expansion of osteolineage "niche" cells initiates or is required for subsequent expansion of functional HSCs.

To further understand the effects of HSC mobilizing treatments on osteoblasts, we next assessed ALP enzymatic activity in these cells during the Cy/G treatment protocol. Whereas bone-specific ALP activity in OPN$^+$ cells isolated from G-CSF only (G2) treated mice was increased compared with osteoblasts harvested from untreated control mice, osteoblasts isolated from D2 Cy/G-treated mice showed lower ALP activity (Figure S3B). Importantly, ALP activity in all OPN$^+$ cell populations was always substantially higher than that of a predominantly hematopoietic negative control population (Figure S3B). Given that ALP activity typically increases as osteolineage cells progress from proliferative preosteoblasts to mature, matrix-secreting osteoblasts,[12,34,35,42] these differences in ALP activity likely reflect differences in the predominant state of osteoblast differentiation in untreated, Cy/G-treated, and G- only treated mice. Increased ALP activity in G-only treated mice is indicative of a shift toward a more differentiated osteoblast population in these animals. In contrast, reduced ALP activity in Cy/G-treated mice indicates the presence of a less differentiated population and is consistent with their increased proliferative activity (Figure 3D), which is typical of less mature osteolineage cells. Thus, in addition to proliferative expansion, osteolineage cells exhibit phenotypic changes in response to Cy/G treatment that could influence the interactions of these niche cells with HSC in mobilized mice.

Mobilizing agents induce changes in osteoblastic niche cells that influence HSC proliferation

In light of the fact that mobilization-induced changes in the osteoblast compartment are apparent before changes in HSCs, we hypothesized that altered osteoblast function may actually initiate changes in the HSC compartment associated with mobilization. To test this hypothesis, we used cell sorting to directly assess the effects of untreated or Cy/G-treated OPN$^+$ cells on isolated HSCs. A total of 100 000 lineage-negative (Lin$^-$) BM cells, which include HSCs and hematopoietic progenitor cells (this Lin$^-$ BM population will be referred to hereafter as "HPC") were exposed for 12 hours in vitro to 2000 OPN$^+$ osteoblasts isolated from untreated mice or from D2 mobilized mice (which had received 1 dose of Cy plus 2 daily doses of G; Figure 4A). The average input HSC frequency in these cultures was 4% plus or minus 1.8% (Figure 4B). After 12 hours, the total frequency of primitive c-Kit$^+$ Thy1.1^{lo}Lineage$^-$Sca-1$^+$ (KTLS) HSCs remaining in each progenitor cell/osteoblast coculture (HPC:osteoblast) was determined by FACS. As shown in Figures 4B and S4A, cocultures containing D2 osteoblasts exhibited an increased frequency of KTLS HSCs

among BM-derived precursors (average frequency, 13% ± 2%, Figure 4B), compared with the frequency of KTLS HSC observed in cocultures containing osteoblasts isolated from untreated mice (6% ± 1%). Interestingly, the frequency of KTLS HSCs observed among BM cells in D2 osteoblast cocultures was similar to that in cultures of HPCs only (ie, Lin$^-$ BM cells cultured 12 hours. in the absence of any osteoblast population), suggesting that untreated, but not D2, OPN$^+$ cells may negatively regulate HSC proliferation in this system. Importantly, nonosteoblastic (OPN$^-$) stromal cells had no effect on the frequency of HSCs in similar coculture experiments (Figure S5).

To further assess the effects of osteoblasts on HSC proliferation, we also used CFSE dilution assays to examine HSC division rates after 36-hour exposure to normal or D2 mobilized OPN$^+$ cells. These assays revealed a striking difference in the rate of CFSE loss among KTLS HSCs exposed to D2 osteoblasts, compared with HSCs in the presence of untreated osteoblasts or HSCs cultured alone. Both the fraction of dividing HSCs and the average number of HSC divisions were substantially higher among HSCs exposed to D2 osteoblasts (Figure 4C,D). As noted, this increased HSC proliferation in the presence of D2 osteoblasts was accompanied by a significant increase in relative frequency and overall numbers of HSCs in D2 osteoblast:HSC cocultures, compared with either untreated osteoblast:HPC or HPC alone cultures (Figures 4B, S4A). Interestingly, transwell assays, in which cell-cell contact between the input osteoblast and hematopoietic populations could be prevented while allowing exposure to secreted/soluble factors, revealed that induction of HSC proliferation by D2 osteoblasts (HPC:D2) does not depend on cell contact, as the fraction of dividing HSC was equivalent in transwell cultures (Figure S4B, transwell, HPC:D2 compare gray filled, transwell to black dotted, nontranswell). In contrast, the negative regulation of HSC proliferation mediated by untreated osteoblasts was at least partially dependent on cell contact, as demonstrated by the increased fraction of dividing HSCs in these cultures when cell contact was disrupted by the transwell filter (Figure S4B, transwell, HPC: untreated compare gray filled to black dotted, $P < .05$).

Next, to determine whether increases in HSC frequency and number in the presence of D2 osteoblasts might be facilitated by enhanced HSC survival in addition to increased proliferation (Figure 4C,D), we measured the frequency of apoptotic HSC (KTLS) in HPC only, HPC:untreated, and HPC:D2 cocultures. HPC apoptosis was measured via cell membrane specific changes in phospholipid-like phosphotidylserine, detected by annexin V. HPCs were cultured alone or exposed to untreated or D2 osteoblasts, for 12 hours, and the frequency of early apoptotic cells (annexin V$^+$) and late apoptotic or necrotic cells (annexin V$^+$, PI$^+$) within the total KTLS HSC population was determined by flow cytometry. This analysis revealed equivalent rates of apoptosis among HSCs exposed to either untreated or D2 osteoblasts (4.5% vs 6% annexin V$^+$, PI$^+$; Figure 4E). Interestingly, we observed significantly fewer apoptotic KTLS HSCs in cultures containing either untreated or D2 osteoblasts, compared with KTLS cells maintained in the absence of osteoblasts (HPC only, 13% annexin V$^+$, PI$^+$; Figure 4E; $P \leq .05$ for HPCs only compared with HPC:untreated and HPCs only compared with HPC:D2). Although a low frequency of early apoptotic cells (annexin V$^+$) could be detected in total cultured cells (data not shown), there were no detectable early apoptotic KTLS cells under any culture conditions tested (Figure 4E). These data indicate that osteoblasts provide an antiapoptotic signal to HSCs ex vivo and that this effect is unaltered by Cy/G treatment. Moreover, these data argue that the increases in
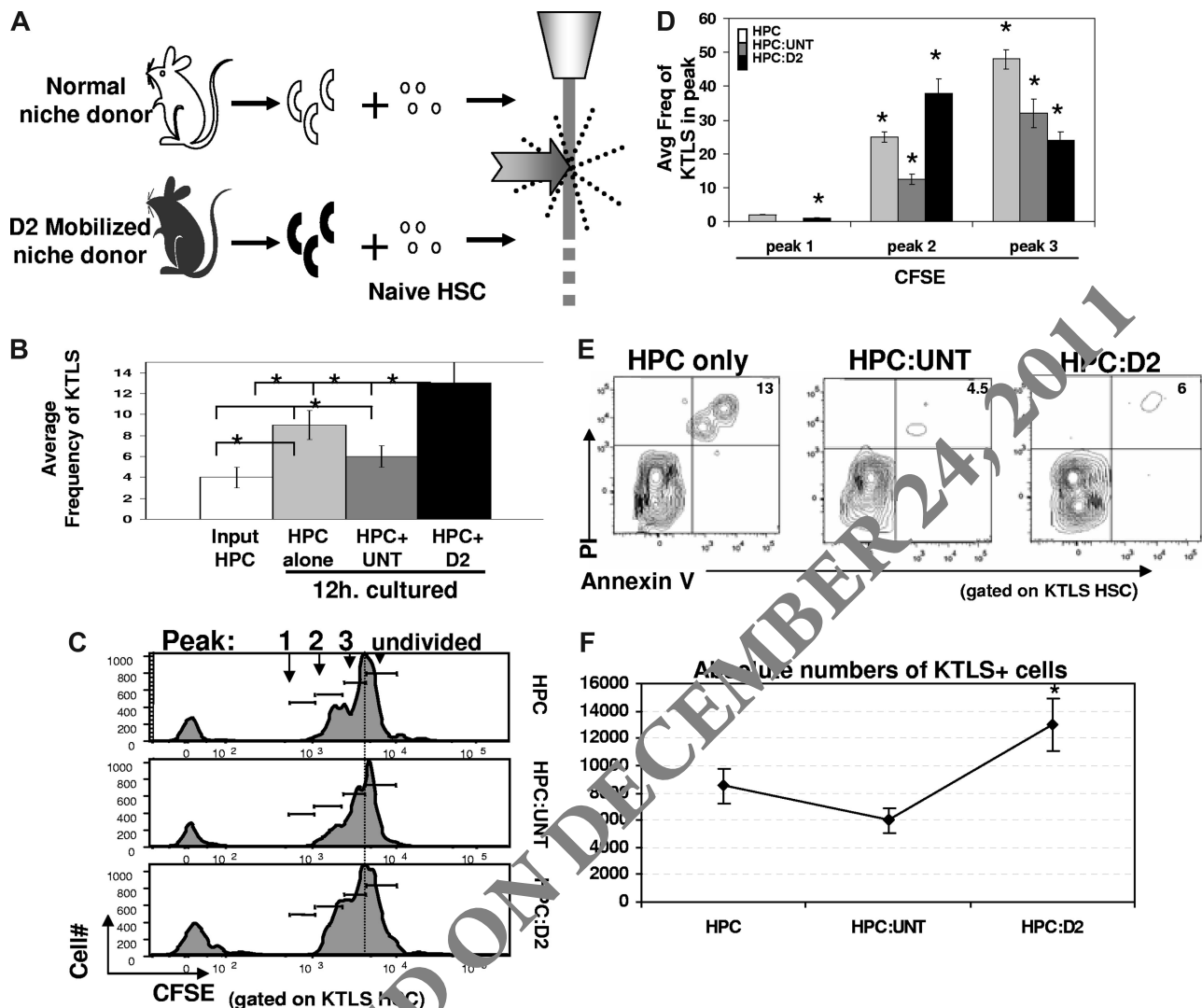
Figure 4. Cytokine mobilized osteoblasts promote HSC proliferation and maintain HSC reconstituting potential. (A) Experimental strategy. A total of 100 000 lineage-negative (Lin⁻) BM cells, which include HSCs and hematopoietic progenitor cells (HPCs) from untreated mice, were exposed for 12 hours in vitro to 2000 OPN⁺ osteoblasts isolated from untreated mice (white) and analyzed for KTLS frequency and/or proliferation by loss of CFSE by FACS. (B) Frequency of c-kit⁺Thy1.1ˡᵒLin⁻Sca1⁺ (KTLS) HSC among Lin-depleted BM (HPC) maintained alone (□) or with untreated (▨) or cytokine-modified (D2; ■) osteoblasts for 12 hours. KTLS HSC frequency among input HPCs is also shown (□). Data are presented as the average frequency of KTLS HSC (± SD) as determined by FACS in short-term (12 hours) HPC:osteoblast cocultures (*P < .05). Data are compiled from 6 independent experiments performed. (C) Increased proliferation of CFSE-labeled KTLS HSC among Lin-depleted BM cells (HPC) cultured with cytokine-modified (HPC:D2, panel 3) compared with untreated (HPC:untreated, panel 2) osteoblasts after 36 hours. Histograms represent CFSE labeling of only those cells falling within the KTLS gate and are representative of 7 independent experiments. (D) Average frequency (± SD) of divided KTLS cells per peak (1, 2, 3, as indicated in panel C) in coculture experiments (*P < .05). (E) Increased cell survival in HPC cultures containing untreated or D2 osteoblast, compared with HPC cultured alone. Cultures were performed as described previously, and stained with KTLS surface markers in addition to markers of cell death and viability (annexin V (early apoptosis marker) and PI (late apoptosis marker)). Data are representative of 2 independent experiments. (F) Increased total numbers of KTLS HSCs in HPC:D2 cultures. HSC numbers were determined for each culture by multiplying the frequency of KTLS cells (determined by FACS) by the total number of cells present. Data are shown as the mean absolute cell number for each condition over 7 independent experiments plus or minus the SD (*P < .05).

KTLS HSC frequency (Figure 4B) and number (Figure 4F) observed in the presence of D2 osteoblasts result from increased HSC proliferation (Figure 4C,D), rather than enhanced survival (Figure 4E). Together with the transwell experiments described herein, these data suggest a model wherein, in the steady state, osteoblasts negatively regulate stem cell expansion through direct contact with HSC, whereas "mobilized" osteoblasts (D2) overcome this inhibition of HSC proliferation by elaboration and/or inhibition of a soluble factor(s) that acts on hematopoietic precursors.

Mobilization induces changes in osteoblastic niche cells that influence HSC function

Osteoblasts have been implicated as important regulators of HSC function.[2,7] A hallmark function of HSC is their capacity to

engraft and reconstitute hematopoiesis in lethally irradiated recipients. To test whether HSC proliferation in the presence of osteoblasts may better support HSC reconstituting activity than HSC proliferation in the absence of osteoblasts (ie, in HPC only cultures), we compared the in vivo hematopoietic engraftment potential of untreated, wild-type HSCs previously exposed for 12 hours only to either untreated or D2 osteoblasts, or to control conditions lacking osteoblasts (Figure 5A). To easily track HSCs and their progeny after transplant, HPCs were isolated from transgenic mice constitutively expressing CFP under the control of the constitutive β-actin promoter.[25,26] CFP⁺ HPCs were incubated for 12 hours with CFP⁻ OPN⁺ cells from either untreated or D2 Cy/G-treated mice, and then transplanted intravenously at equal cell numbers (5000 HPCs/mouse) into
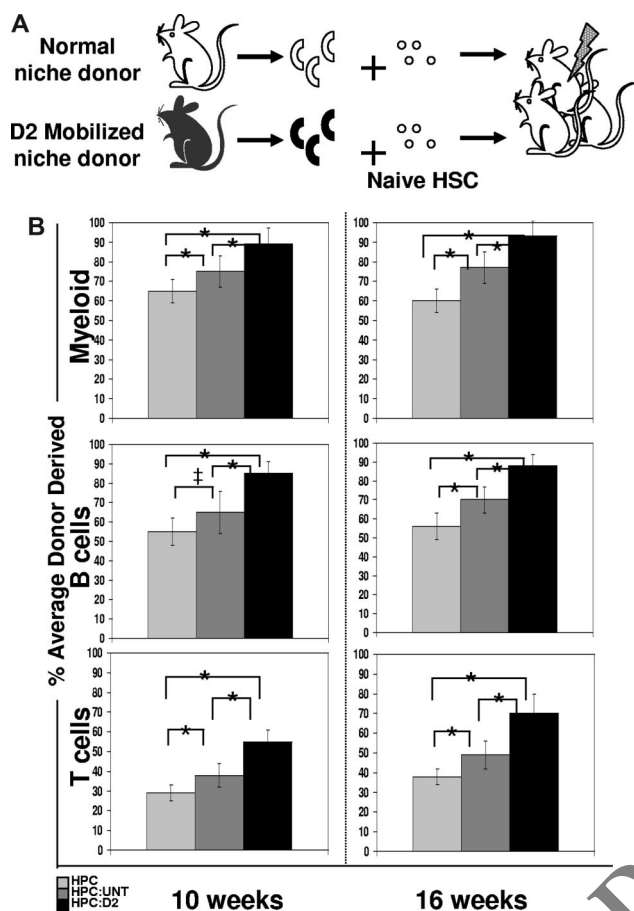
Figure 5. Increased engraftment efficiency of CFP⁺ HSC exposed for 12 hours to D2 osteoblasts compared with HSC exposed to untreated osteoblasts.
(A) Experimental strategy. A total of 100 000 Lin⁻ BM cells (HPC) from untreated mice were exposed for 12 hours in vitro to 2000 OPN⁺ osteoblasts isolated from D2 mobilized mice (which had received 1 dose of Cy + 2 daily doses of G; black) and tested for HSC function by measuring reconstitution potential. (B) Lethally irradiated recipient mice were transplanted with cells from 12-hour HPC only cultures (▨), or HPC:untreated (▨) or HPC:D2 (■) cocultures. The average engraftment was calculated by determining the percentage donor-derived myeloid (top; Mac-1⁺, Gr-1⁺), B (middle, B220⁺), and T (bottom, CD3⁺, CD4⁺, CD8⁺) cells at the indicated time points after transplant. Donor-derived cells were identified based on CFP transgene expression and were corrected for the percentage of CFP⁺ myeloid or lymphoid populations (80%-90%) in unmodified CFP⁺ transgenic hosts (*$P < .05$; ‡$P = .0598$). Error bars represent SD.

lethally irradiated CFP⁺ recipients. The hematopoietic repopulating activity of HSCs contained within the transplanted HPCs was assessed at 4, 6, 8, 10, and 16 weeks after transplantation by flow cytometric analysis of donor-derived (CFP⁺) myeloid and mature B and T cells in the recipients' peripheral blood. At all time points tested, recipient mice transplanted with HPCs that had been exposed previously to D2 osteoblasts showed more robust myeloid (Mac-1⁺, Gr-1⁺), B (B220⁺), and T (CD3⁺, CD4⁺, CD8⁺) cell engraftment than did HSCs from either untreated osteoblast cocultures or HSCs maintained alone before transplant (Figure 5B and data not shown; compare black [HPC exposed to D2 osteoblasts] to dark gray [HPC exposed to untreated osteoblast] and light gray [HPC only] bars). Whereas HSCs derived from HPC:untreated cultures exhibited a less robust engraftment potential than those from HPC:D2 cultures, the engraftment potential in this population was still enhanced compared with hematopoietic reconstitution in mice transplanted with cells from HPC only cultures (Figure 5B light gray bar). Thus, these transplantation assays demonstrate a graded

ability of these different conditions to maintain or expand HSC activity, with the level of HSC activity highest among cells exposed to D2 OPN⁺ cells, lower among cells exposed to untreated osteoblasts, and lowest among cells cultured in the absence of osteoblasts. Because engraftment potential is a direct measure of HSC activity, the increased hematopoietic reconstitution in D2-transplanted mice (Figure 5B), combined with the increased frequency and proliferation of KTLS HSC (Figure 4B-D), suggests that D2 osteoblasts directly promote HSC proliferation while maintaining HSC self-renewal and functional activity.

ATM mediates the mobilization-induced changes in osteoblastic niche cells that influence HSC proliferation and function

The preceding data clearly indicate that osteolineage cells, prospectively isolated fresh from the bone, can directly communicate with HSCs and modulate their function in response to physiologic stimuli, such as mobilization. To better understand the molecular mechanisms involved in mobilization-induced changes in the osteoblastic niche, we sought to determine which signaling pathways might be essential to mediate Cy/G-induced increases in osteoblast proliferation and HSC support function. In surveying the existing literature, we became particularly interested in the potential role of the "ataxia telangiectasia mutated" (*Atm*) gene. *Atm* encodes a protein Ser/Thr kinase that helps to maintain genomic stability by activating proteins involved in the G₁/S and G₂/M cell cycle checkpoints in response to DNA damage, telomeric instability, or oxidative stress.[52,53] Studies of *Atm*⁻/⁻ (ATM KO) mice have implicated this kinase both in the intrinsic maintenance of HSC self-renewal and in the maintenance of appropriate bone mass in vivo[21,22,24]; however, whether these represent completely independent or linked biologic roles of ATM has not been clear. Thus, in light of the activity of ATM in both blood and bone cells, and in cellular responses to DNA damage and oxidative stress (such as occurs in the context of cell death induced by Cy treatment[52-54]), we hypothesized that ATM may additionally function in regulating intercellular communication between osteoblasts and HSCs.

To first understand whether ATM-dependent signals are important in regulating mobilization-induced changes in the osteoblastic niche, we analyzed the frequency and absolute numbers of OPN⁺ cells in untreated or Cy/G mobilized *Atm*⁺/⁺ (wild-type, WT) or *Atm*⁻/⁻ (knockout, KO) mice. As expected, the frequency and absolute numbers of osteoblasts increased dramatically in mobilized D2 *Atm*⁺/⁺ compared with untreated *Atm*⁺/⁺ mice (frequency 60% ± 7% vs 20% ± 10%, $P = .039$, data not shown; absolute numbers 28 000 ± 5000 vs 7500 ± 1200, $P < .05$; Figure 6A). However, in *Atm*⁻/⁻ mice, we observed a slight difference in the overall frequency of OPN⁺ cells but no change in the absolute numbers of OPN⁺ osteoblasts in response to Cy/G treatment (frequency, 30% ± 7% vs 41% ± 6%, $P = .047$, data not shown; total numbers, 8600 ± 1100 vs 11 000 ± 1300, no significant difference; Figure 6A). The failure of mobilization to substantially alter the frequency and number of osteoblastic niche cells in *Atm*⁻/⁻ mice can at least in part be attributed to an increased rate of apoptosis among freshly isolated OPN⁺ cells from mobilized *Atm*⁻/⁻ mice (ATM KO D2, 12% ± 3% annexin V⁺, PI⁺ cells), compared with OPN⁺ cells from WT mobilized mice (ATM WT D2, 5% ± 1.4% annexin V⁺, PI⁺ cells; Figure 6B, $P = .049$). Thus, these data indicate that mobilization-induced expansion of osteoblastic niche cells depends on the function of ATM kinase to promote osteoblast survival (Figure 6A,B).
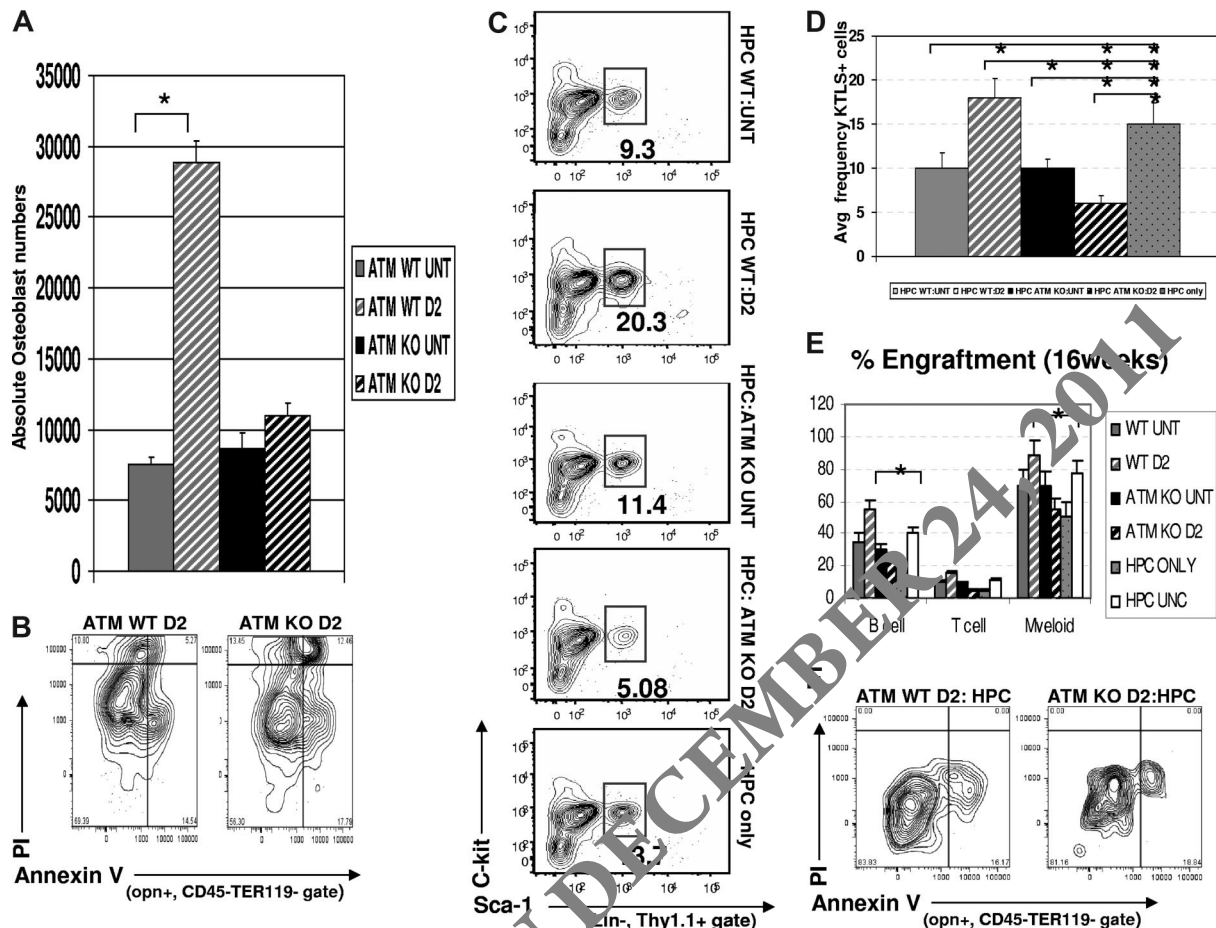
Figure 6. Effects of Cy/G treatment in *ATM⁻/⁻* mice. (A) Osteoblast numbers are not increased in Cy/G treated ATM-deficient mice. The total numbers of osteoblasts isolated after Cy/G treatment were calculated based on the frequency of OPN⁺ cells (as determined by FACS) among total numbers of cells isolated from collagenase treated bones from either *ATM⁺/⁺* or *ATM⁻/⁻* mice that were untreated (ATM WT untreated, ▨; ATM KO untreated, ■) or treated with Cy/G (ATM WT D2, gray hatched; ATM KO D2, black hatched). Data are plotted as means ± SD (*P < .05). (B) Decreased osteoblast survival after Cy/G treatment in ATM-deficient mice. ATM WT or ATM KO mice were treated with Cy/G and osteoblasts were isolated from collagenase-treated bones and stained with osteoblast specific markers as well as cell viability markers (annexin V⁺, early apoptotic marker; and PI⁺, late apoptotic marker). Representative data for 2 independent experiments are shown. (C-E) Lower frequency and engraftment efficiency of wild-type HSC exposed for 12 hours to D2 ATM KO osteoblasts compared with HSC exposed to wild-type D2 osteoblasts. A total of 100,000 Lin⁻ BM cells (HPC) from wild-type, untreated mice were exposed for 12 hours in vitro to 20,000 OPN⁺ osteoblasts isolated from ATM KO or WT D2 mobilized mice (ATM WT untreated, ▨; ATM KO untreated, ■; ATM KO D2, black hatched; ATM WT D2, gray hatched) and tested for HSC function by measuring in vitro maintenance of HSC frequency (C,D) compared with an HPC only control (gray dotted bar in panel D) and in vivo reconstitution potential (E) as described previously (Figures 4,5). Data are shown compared with an HPC only control (gray dotted) and an uncultured HPC control (▨). Data are plotted as mean (± SD; *P < .05) and represent chimerism at 16 weeks after transplant. (F) Equivalent frequency of apoptotic (annexin V⁺, PI⁻ early apoptotic) osteoblasts after 12-hour HPC:osteoblast coculture assays. Coculture assays were performed as described previously, and cells were stained for osteoblast specific markers and the cell death and viability markers annexin V (early apoptotic marker) and PI (late apoptotic marker). Representative data are shown for 2 independent experiments performed.

To address whether ATM may play an additional role in the mobilization-responsive regulation of HSC proliferation and reconstitution activity by osteoblasts, we next assessed the effects of untreated or Cy/G-treated OPN⁺ cells isolated from either *Atm⁺/⁺* or *Atm⁻/⁻* mice on the frequency and engraftment potential of WT naive HSCs (functionally replete for ATM and never exposed to Cy or G). Using short-term (12 hours) in vitro coculture assays identical to those described in "Cell culture and proliferation assays," we determined that WT HPCs exposed to D2 osteoblasts from *Atm* KO mice (HPC: ATM KO D2) exhibited a reduced frequency of KTLS HSCs among BM-derived precursors (average frequency, 5% ± 1.5%, Figure 6C,D), compared with that observed in cocultures containing WT D2 osteoblasts (HPC:WT D2; 18% ± 2.1%, P < .05) or to untreated control cocultures containing untreated osteoblasts isolated from either *Atm* WT or *Atm* KO animals (HPC:WT untreated, 10% ± 2.8%, P < .05; HPC:KO untreated, 11% ± 1.3%, P < .05). Importantly, the difference in the ability of osteoblasts isolated from *Atm* WT vs *Atm* KO

Cy/G-treated (D2) mice to maintain HSCs in coculture assays was not the result of loss of *Atm* KO osteoblasts via increased apoptosis. No OPN⁺ apoptotic cells (annexin V⁺, PI⁺) and only a low and equivalent frequency of pre-apoptotic cells (annexin V⁺, PI⁻) could be detected in a comparison of *Atm* WT D2 OPN⁺ cells (16% ± 3% annexin V⁺, PI⁻) and *Atm* KO D2 OPN⁺ cells (18% ± 1% annexin V⁺, PI⁻) after 12 hours of culture (Figure 6F, P = .037).

To confirm that the decreased HSC frequency among HPCs exposed to *Atm* KO osteoblasts represents a decrease in the maintenance of functional HSCs, we also compared the in vivo hematopoietic engraftment potential of untreated, WT HPC exposed for 12 hours to equal numbers of either *Atm* KO D2 osteoblasts (HPC:ATM KO D2) or WT D2 osteoblasts (HPC:WT D2), or to control conditions (HPC:WT untreated; HPC:ATM KO untreated; HPC only). In addition, in these studies, we also compared HSC engraftment after in vitro exposure to sorted

OPN+ cells to engraftment from freshly isolated, uncultured HPCs (HPC UNC).

As in previous experiments, WT HPCs exposed to WT D2 osteoblasts showed significantly greater hematopoietic engraftment potential than HPCs exposed to WT untreated osteoblasts. Indeed, reconstitution by HPCs exposed to WT D2 osteoblasts exceeded that of an equivalent number of freshly isolated (uncultured) HPCs, indicating that exposure to WT D2 osteoblasts indeed expands functional HSCs ex vivo (Figure 6E, compare white vs gray striped bars, $P < .05$ for myeloid and B cell). In contrast, as predicted from frequency analysis (Figure 6C), recipient mice transplanted with HPCs exposed previously to *Atm* KO D2 osteoblasts (ATM KO D2) showed approximately 2-fold lower reconstitution of both myeloid and lymphoid lineages compared with HPCs exposed to WT D2 osteoblasts ($55\% \pm 7\%$ vs $89\% \pm 9\%$ for myeloid cells, $P < .05$, and $25\% \pm 2\%$ vs $55\% \pm 5.5\%$ for B cells, $P < .05$). The engraftment potential of WT HPCs exposed to *Atm* KO D2 osteoblasts was no greater than that of HPCs exposed to untreated *Atm* KO osteoblasts, to uncultured HPCs, or to HPCs cultured alone (Figure 6E). Because multilineage engraftment potential is a direct measure of HSC activity, this decreased hematopoietic reconstitution in mice transplanted with HPCs exposed to *Atm* KO osteoblasts (Figure 6E), combined with the decreased frequency of KTLS HSC in cultures containing *Atm* KO osteoblasts (Figure 6C) and the equivalent rate of survival of *Atm* WT and *Atm* KO osteoblasts in culture (Figure 6E), suggests that ATM plays a key role in the alteration of osteoblast function that normally accompanies Cy/G treatment and that enables D2-mobilized osteoblasts to promote HSC proliferation (Figure 4) and expansion of reconstituting activity (Figure 5).

Discussion

Recent studies implicate osteoblasts as an important cellular component of the HSC niche.[3,8,55-58] These studies demonstrate that, in mouse models displaying increased osteoblast cell numbers, there is a concomitant enhancement in the ability of BM-derived mixed stroma cultures to support hematopoiesis[2,7,58] and an increase in vivo in long-term reconstituting HSCs.[6] Although these findings suggest that limited availability of osteoblasts may normally limit stem cell expansion, discrimination of the direct versus indirect effects of osteoblasts on HSC numbers and activity is complicated in these studies by the unavoidable presence of other microenvironmental inputs in the complex cellular milieu of the bone marrow. These issues have spurred significant controversy regarding the particular contribution of the osteoblastic HSC niche, particularly in light of recent suggestions that vascular endothelial cells may provide an "alternative" niche for HSCs.[5,14] Thus, to assay the specific contributions of osteoblasts to the HSC niche and their role in the regulation of HSC number and function, we directly isolated these putative niche components and directly tested their effect on HSC function. This approach deconstructs the complexity of the marrow environment to ask specifically whether osteoblasts are alone sufficient to regulate HSC activity.

To identify and isolate osteoblasts fresh from the bone, we used enzymatic digestion coupled with positive and negative selection to specifically purify a population of OPN+CD45−Ter119− cells that is highly enriched for osteoblast-specific markers and bone-forming activity. This efficient and reliable approach to acquire osteolineage cells for study allows the direct analysis of osteoblasts and abrogates the need for extensive cell culture, which can

profoundly alter cellular activity. In addition, this strategy allows rapid enumeration of the frequency and number of osteoblasts in vivo, as well as direct assessment of changes in their phenotypic and functional properties under particular in vivo conditions. (It is important to note that, whereas sorted OPN+ cells appear largely homogeneous based on phenotypic [Figures 1,S2] and functional [Figure 2] analyses, because these cells do not survive at clonal density [data not shown], we cannot exclude the possibility that additional, rare cell populations copurify with OPN+ cells and may contribute to their activity.) Nonetheless, this novel prospective isolation approach will be advantageous for a variety of future analyses aimed at understanding the activity of osteolineage cells in different physiologic states relevant to both normal and pathologic hematopoiesis and bone development.

Making use of this direct osteoblast identification and isolation strategy, we examined the role of osteolineage cells in the clinically relevant induced expansion of HSC that occurs in response to Cy/G treatment. We found that osteoblast numbers and frequency increase significantly in response to Cy/G mobilization. Importantly, expansion of the osteoblastic niche precedes Cy/G-induced HSC expansion, suggesting that osteoblasts may indeed initiate HSC proliferation during stem cell mobilization. Consistent with this notion, osteoblasts isolated from Cy/G-treated mice enhanced the proliferation of naive (unmobilized) HSCs in short-term coculture assays, compared with osteoblasts isolated from untreated animals. Moreover, in vivo transplantation of HPCs exposed to osteoblasts from Cy/G-treated versus untreated mice additionally indicated that mobilization-induced changes in the functional interactions of osteoblasts with HSCs directly impact the ability of these cells to maintain hematopoietic reconstituting capacity. Significantly, the molecular mechanism underlying these changes in osteoblast number and function could be traced to the ATM signaling pathway, demonstrating a new role for this kinase in supporting stem cell niche activity. The studies presented here thus provide the first demonstration that changes that occur within the in vivo osteoblastic niche during Cy/G-induced HSC mobilization are sufficient to directly modify HSC function. These data substantiate the role of osteoblasts as HSC niche cells and further advance our understanding of the activity of the osteoblastic niche by demonstrating that (1) direct communication between osteoblasts and HSCs is itself sufficient to induce physiologically relevant changes in HSC function, (2) this communication is responsive to physiologic cues (such as mobilizing stimuli), and (3) this communication can involve both cell-cell contact and soluble signals elaborated by osteoblasts.

Taken together, our data are consistent with a model (Figure 7) in which Cy/G mobilization induces functional changes in the interactions of osteoblastic niche cells with HSCs, and these changes in turn directly alter HSC activity. Whereas, in the absence of osteoblasts, HSCs proliferate in a manner that leads to loss of functional reconstituting activity (probably the result of unchecked HSC differentiation[44,59,60]), when exposed to untreated osteoblasts, stem cell proliferation is diminished, and these cells retain reconstituting potential (Figure 5). Thus, normal osteoblasts appear to maintain HSC function in part by holding them in a quiescent state.[43,59,61] This restriction of HSC proliferation appears to depend on direct cell-cell contact between the HSC and its niche (Figure S4B). In contrast, when exposed to HSC-mobilizing agents, the osteoblastic niche undergoes dramatic changes. These cells expand significantly, exhibit changes in enzymatic activity consistent with alterations in their differentiation state (Figures 3,S3), and
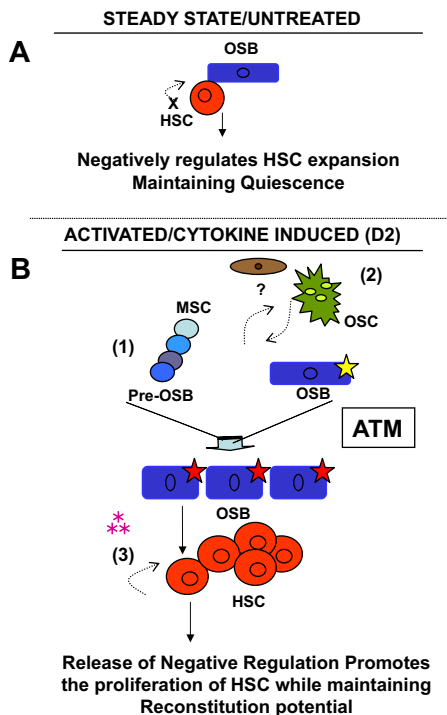
Figure 7. Model of osteoblast-mediated HSC mobilization and maintenance of reconstituting potential. (A) Osteoblasts (blue) within the normal BM microenvironment appear to negatively regulate HSC proliferation (red), at least in part through cell-cell contact. (B) Changes in the osteoblast compartment induced by Cy/G treatment (indicated by yellow star) alter the niche (red star) such that osteoblasts promote HSC proliferation and maintain HSC reconstitution potential. This alteration could arise in vivo directly, by regulation of fully differentiated osteoblasts by Cy/G, or indirectly, via (1) the stimulation/proliferation of more primitive osteoprogenitor cells (blue) or (2) the cross-regulation/activation of osteoblasts by osteoclasts (green) or other stromal elements (brown), that through an ATM dependent mechanism results in (3) a specialized subset of osteolineage cells that are sufficient to promote HSC self-renewal through the secretion of soluble factors (pink asterisks).

elaborate soluble factors that directly promote HSC proliferation (Figures 4,S4) while maintaining their functional reconstituting potential (Figure 5). Interestingly, the specific mobilization-induced changes in osteoblast number and function that result from Cy/G treatment (including osteoblast expansion and osteoblast-mediated support of HSC proliferation) are absent in animals lacking ATM (Figure 6).

In conclusion, these data demonstrate that the osteoblast population present in Cy/G-treated mice is both phenotypically and functionally distinct from its steady-state counterpart and that changes in the osteoblastic niche, including the ability to support and maintain HSC function, are mediated at least in part by ATM, implicating DNA damage and oxidative stress pathways activated in osteolineage niche cells in the induction of HSC expansion in response to Cy/G. This study thus provides new insight into the cellular and molecular mechanisms underlying the clinically important process of HSC mobilization. In addition, the fact that freshly purified osteoblasts can act autonomously in culture to communicate physiologically appropriate regulatory signals to HSC presents a new and powerful opportunity for direct interrogation of the interactions of stem cells with their niche and for future discovery of novel genes and pathways important in maintaining optimal and appropriate stem cell function. These data will have important future implications for strategies to induce stem cell expansion ex vivo and in the context of bone marrow transplantation.

Acknowledgments

Authorship

Contribution: S.R.M. and A.J.W. designed and interpreted the experiments; S.R.M. performed the experiments; S.R.M. and A.J.W. wrote and edited the manuscript.

Conflict-of-interest disclosure: The authors declare no competing financial interests.

Correspondence: Amy J. Wagers, Joslin Diabetes Center, One Joslin Place, Room 620C, Boston, MA 02215; e-mail: amy.wagers@joslin.harvard.edu.

References

1. Kondo M, Wagers AJ, Manz MG, et al. Biology of hematopoietic stem cells and progenitors: implications for clinical application. Annu Rev Immunol. 2003;21:759-806.

2. Zhang J, Niu C, Ye L, Huang H, et al. Identification of the haematopoietic stem cell niche and control of the niche size. Nature. 2003;425:836-841.

3. Zhu J, Emerson SG. A new bone to pick: osteoblasts and the haematopoietic stem-cell niche. Bioessays. 2004;26:595-599.

4. Nilsson SK, Johnston HM, Coverdale JA. Spatial localization of transplanted hemopoietic stem cells: inferences for the localization of stem cell niches. Blood. 2001;97:2293-2299.

5. Kiel MJ, Morrison SJ. Maintaining hematopoietic stem cells in the vascular niche. Immunity. 2006;25:862-864.

6. Calvi LM, Adams GB, Weibrecht KW, et al. Os-

teoblastic cells regulate the haematopoietic stem cell niche. Nature. 2003;425:841-846.

7. Balduino A, Hurtado SP, Frazão P, et al. Bone marrow subendosteal microenvironment harbours functionally distinct haemosupportive stromal cell populations. Cell Tissue Res. 2005;319:255-266.

8. Stier S, Forkert R, Lutz C, et al. Osteopontin is a hematopoietic stem cell niche component that negatively regulates stem cell pool size. J Exp Med. 2005;201:1781-1791.

9. Calvi LM, Sims NA, Hunzelman JL, et al. Activated parathyroid hormone/parathyroid hormone-related protein receptor in osteoblastic cells differentially affects cortical and trabecular bone. J Clin Invest. 2001;107:277-286.

10. Bakker A, Klein-Nulend J. Osteoblast isolation from murine calvariae and long bones. Methods Mol Med. 2003;80:19-28.

11. Jonsson KB, Frost A, Nilsson O, Ljunghall S,

Ljunggren O. Three isolation techniques for primary culture of human osteoblast-like cells: a comparison. Acta Orthop Scand. 1999;70:365-373.

12. Quarles LD, Yohay DA, Lever LW, Caton R, Wenstrup RJ. Distinct proliferative and differentiated stages of murine MC3T3-E1 cells in culture: an in vitro model of osteoblast development. J Bone Miner Res. 1992;7:683-692.

13. Adams GB, Martin RP, Alley IR, et al. Therapeutic targeting of a stem cell niche. Nat Biotechnol. 2007;25:238-243.

14. Kiel MJ, Yilmaz OH, Iwashita T, Terhorst C, Morrison SJ. SLAM family receptors distinguish hematopoietic stem and progenitor cells and reveal endothelial niches for stem cells. Cell. 2005;121:1109-1121.

15. Sugiyama T, Kohara H, Noda M, Nagasawa T. Maintenance of the hematopoietic stem cell pool by CXCL12-CXCR4 chemokine signaling in bone

marrow stromal cell niches. Immunity. 2006;25: 977-988.

16. Shackelford RE, Innes CL, Sieber SO, Heinloth AN, Leadon SA, Paules RS. The Ataxia telangiectasia gene product is required for oxidative stress-induced G1 and G2 checkpoint function in human fibroblasts. J Biol Chem. 2001;276:21951-21959.

17. Chen K, Albano A, Ho A, Keaney JF Jr. Activation of p53 by oxidative stress involves platelet-derived growth factor-beta receptor-mediated ataxia telangiectasia mutated (ATM) kinase activation. J Biol Chem. 2003;278:39527-39533.

18. Heinloth AN, Shackelford RE, Innes CL, et al. ATM-dependent and -independent gene expression changes in response to oxidative stress, gamma irradiation, and UV irradiation. Radiat Res. 2003;160:273-290.

19. Shoelson SE. Banking on ATM as a new target in metabolic syndrome. Cell Metab. 2006;4:337-338.

20. Hofseth LJ, Saito S, Hussain SP, et al. Nitric oxide-induced cellular stress and p53 activation in chronic inflammation. Proc Natl Acad Sci U S A. 2003;100:143-148.

21. Rasheed N, Wang X, Niu QT, Yeh J, Li B. Atm-deficient mice: an osteoporosis model with defective osteoblast differentiation and increased osteoclastogenesis. Hum Mol Genet. 2006;15:1938-1948.

22. Ito K, Hirao A, Arai F, et al. Reactive oxygen species act through p38 MAPK to limit the lifespan of hematopoietic stem cells. Nat Med. 2006;12:446-451.

23. Hishiya A, Ito M, Aburatani H, Motoyama N, Ikeda K, Watanabe K. Ataxia telangiectasia mutated (Atm) knockout mice as a model of osteopenia due to impaired bone formation. Bone. 2005;37:497-503.

24. Ito K, Hirao A, Arai F, et al. Regulation of oxidative stress by ATM is required for self-renewal of haematopoietic stem cells. Nature. 2004;431:997-1002.

25. Hadjantonakis AK, Nagy A. The color of mice: in the light of GFP-variant reporters. Histochem Cell Biol. 2001;115:49-58.

26. Hadjantonakis AK, Macmaster S, Nagy A. Embryonic stem cells and mice expressing different GFP variants for multiple non-invasive reporter usage within a single animal. BMC Biotechnol. 2002;2:11.

27. Telford WG, Cox WG, Stiner D, Singer VL, Doty SB. Detection of endogenous alkaline phosphatase activity in intact cells by flow cytometry using the fluorogenic ELF-97 phosphatase substrate. Cytometry. 1999;37:314-319.

28. Morrison SJ, Wright DE, Weissman IL. Cyclophosphamide/granulocyte colony-stimulating factor induces hematopoietic stem cells to proliferate before mobilization. Proc Natl Acad Sci U S A. 1997;94:1908-1913.

29. Wergedal JE, Baylink DJ. Characterization of cells isolated and cultured from human bone. Proc Soc Exp Biol Med. 1984;176:60-69.

30. Li V, Raouf A, Kitching R, Seth A. Ets2 transcription factor inhibits mineralization and affects target gene expression during osteoblast maturation. In Vivo. 2004;18:517-524.

31. Kitching R, Qi S, Li V, et al. Coordinate gene expression patterns during osteoblast maturation and retinoic acid treatment of MC3T3-E1 cells. J Bone Miner Metab. 2002;20:269-280.

32. Raouf A, Ganss B, McMahon C, Vary C, Roughley PJ, Seth A. Lumican is a major proteoglycan component of the bone matrix. Matrix Biol. 2002;21:361-367.

33. Raouf A, Seth A. Discovery of osteoblast-associated genes using cDNA microarrays. Bone. 2002;30:463-471.

34. Raouf A, Seth A. Ets transcription factors and targets in osteogenesis. Oncogene. 2000;19:6455-6463.

35. Vary CP, Li V, Raouf A, et al. Involvement of Ets transcription factors and targets in osteoblast differentiation and matrix mineralization. Exp Cell Res. 2000;257:213-222.

36. Raouf A, Li V, Kola I, Watson DK, Seth A. The Ets1 proto-oncogene is upregulated by retinoic acid: characterization of a functional retinoic acid response element in the Ets1 promoter. Oncogene. 2000;19:1969-1974.

37. Haylock DN, Nilsson SK. Osteopontin: a bridge between bone and blood. Br J Haematol. 2006;134:467-474.

38. Marom R, Shur I, Solomon R, Benayahu D. Characterization of adhesion and differentiation markers of osteogenic marrow stromal cells. J Cell Physiol. 2005;202:41-48.

39. Pockwinse SM, Wilming LG, Conlon DM, Stein GS, Lian JB. Expression of cell growth and bone specific genes at single cell resolution during development of bone tissue-like organization in primary osteoblast cultures. J Cell Biochem. 1992;49:310-323.

40. Fermor B, Skerry TM. PTH/PTHrP receptor expression on osteoblasts and osteocytes but not resorbing bone surfaces in growing rats. J Bone Miner Res. 1995;10:1935-1943.

41. Kalajzic I, Kalajzic Z, Kaliterna M, et al. Use of type I collagen green fluorescent protein transgenes to identify subpopulations of cells at different stages of the osteoblast lineage. J Bone Miner Res. 2002;17:15-25.

42. Stewart K, Walsh S, Screen J, et al. Further characterization of cells expressing STRO-1 in cultures of adult human bone marrow stromal cells. J Bone Miner Res. 1999;14:1345-1356.

43. Bradford GB, Williams B, Rossi R, Bertoncello I. Quiescence, cycling, and turnover in the primitive hematopoietic stem cell compartment. Exp Hematol. 1997;25:445-453.

44. Passegue E, Wagers AJ, Giuriato S, Anderson WC, Weissman IL. Global analysis of proliferation and cell cycle gene expression in the regulation of hematopoietic stem and progenitor cell fates. J Exp Med. 2005;202:1599-1611.

45. Wright DE, Wagers AJ, Gulati AP, Johnson FL, Weissman IL. Physiological migration of hematopoietic stem and progenitor cells. Science. 2001;294:1933-1936.

46. Wright DE, Cheshier SH, Wagers AJ, Randall TD, Christensen JL, Weissman IL. Cyclophosphamide/granulocyte colony-stimulating factor causes selective mobilization of bone marrow hematopoietic stem cells into the blood after M phase of the cell cycle. Blood. 2001;97:2278-2285.

47. Neben S, Marcus K, Mauch P. Mobilization of hematopoietic stem and progenitor cell subpopulations from the marrow to the blood of mice following cyclophosphamide and/or granulocyte colony-stimulating factor. Blood. 1993;81:1960-1967.

48. Papayannopoulou, T. Hematopoietic stem/progenitor cell mobilization: a continuing quest for etiologic mechanisms. Ann N Y Acad Sci. 1999;872:187-197; discussion 197-199.

49. Semerad CL, Christopher MJ, Liu F, et al. G-CSF potently inhibits osteoblast activity and CXCL12 mRNA expression in the bone marrow. Blood. 2005;106:3020-3027.

50. Katayama Y, Battista M, Kao WM, et al. Signals from the sympathetic nervous system regulate hematopoietic stem cell egress from bone marrow. Cell. 2006;124:407-421.

51. Drize N, Chertkov J, Zander A. Hematopoietic progenitor cell mobilization into the peripheral blood of mice using a combination of recombinant rat stem cell factor (rrSCF) and recombinant human granulocyte colony-stimulating factor (rhG-CSF). Exp Hematol. 1995;23:1180-1186.

52. Manda K, Bhatia AL. Prophylactic action of melatonin against cyclophosphamide-induced oxidative stress in mice. Cell Biol Toxicol. 2003;19:367-372.

53. Bhatia AL, Manda K, Patni S, Sharma AL. Prophylactic action of linseed (Linum usitatissimum) oil against cyclophosphamide-induced oxidative stress in mouse brain. J Med Food. 2006;9:261-264.

54. Sivakumar V, Niranjali Devaraj S. Protective effect of Plumbago zeylanica against cyclophosphamide-induced genotoxicity and oxidative stress in Swiss albino mice. Drug Chem Toxicol. 2006;29:279-288.

55. Arai F, Hirao A, Ohmura M, et al. Tie2/angiopoietin-1 signaling regulates hematopoietic stem cell quiescence in the bone marrow niche. Cell. 2004;118:149-61.

56. Visnjic D, Kalajzic I, Gronowicz G, et al. Conditional ablation of the osteoblast lineage in Col2.3deltatk transgenic mice. J Bone Miner Res. 2001;16:2222-2231.

57. Bruserud O, Ryningen A, Wergeland L, Glenjen NI, Gjertsen BT. Osteoblasts increase proliferation and release of pro-angiogenic interleukin 8 by native human acute myelogenous leukemia blasts. Haematologica. 2004;89:391-402.

58. Jung Y, Wang J, Havens A, et al. Cell-to-cell contact is critical for the survival of hematopoietic progenitor cells on osteoblasts. Cytokine. 2005;32:155-162.

59. Fleming WH, Alpern EJ, Uchida N, Ikuta K, Spangrude GJ, Weissman IL. Functional heterogeneity is associated with the cell cycle status of murine hematopoietic stem cells. J Cell Biol. 1993;122:897-902.

60. Carlesso N, Aster JC, Sklar J, Scadden DT. Notch1-induced delay of human hematopoietic progenitor cell differentiation is associated with altered cell cycle kinetics. Blood. 1999;93:838-848.

61. Glimm H, Oh IH, Eaves CJ. Human hematopoietic stem cells stimulated to proliferate in vitro lose engraftment potential during their S/G(2)/M transit and do not reenter G(0). Blood. 2000;96:4185-4193.